Proceedings of the 2009 IEEE International Conference on Systems, Man, and Cybernetics
San Antonio, TX, USA - October 2009

Generating Locomotion for Biped Robots based on the Dynamic Passivization of Joint Control

Minoru Ishida*, Shohei Kato*, Masayoshi Kanoh†, and Hidenori Itoh†
*Department of Computer Science and Engineering, Nagoya Institute of Technology
Gokiso-cho, Showa-ku, Nagoya 466-8555, Japan
Email: {ishida, shohey, itoh}@juno.ics.nitech.ac.jp
†Department of Mechanics and Information Technology, Chukyo University
101 Tokodachi, Kaizu-cho, Toyota 470-0393, Japan
Email: mkanoh@sist.chukyo-u.ac.jp

***Abstract*—A central pattern generator (CPG) and passive dynamic walking (PDW) have attracted much attention in the research field of bipedal locomotion. We describe a motion control method based on dynamic joint passivization for biped robot locomotion. CPG-based motion control is effective for walking on uneven terrain. However, it has serious problems with energy loss. In contrast, PDW saves energy because a robot can walk without any active control or energy input on a downhill slope. However, PDW robot can not walk on uneven terrian, but only on a downhill slope. We think that active walking needs to be mixed with PDW for robot walking. Our motion control method is based on a mixture of the CPG and PDW, that is, the dynamic passivization of joint control. Experiments using the motion control method based on dynamic passivization of joint control successfully generated energy efficient walking and enabled superior gaits.**

***Index Terms*—Biped Robot, Central Pattern Generator, Passive Dynamic Walking, Dynamic Passivization of Joint Control, Downhill slope**

I. INTRODUCTION

A lot of research on humanoid robots or biped robots has been conducted. This research focused on enabling robots to walk very smoothly, similar to the way humans walk, which is highly energy efficient. Motion control using a central pattern generator (CPG) has attracted much attention as an effective control mechanism for biped robots to achieve human-like walking (e.g., [1]–[7]). The CPG is modeled mathematically to a neural rhythm generator that exists at a relatively low level of the central nervous system, such as the spinal cord of animals. This motion control using the CPG has generated various motions: walking [1]–[5], step [6], and drum motions [7]. Taga [2], [3] proposed a neuro-musculo-skeletal model based on the CPG, and it enabled a biped robot to have a human gait in two dimensions. Among the researchers of highly energy-efficient walking, McGeer [8] was the first to study passive dynamic walking (PDW). A PDW robot walks forward by placing the foot on the ground and riding on the supporting leg, which rolls forward as an inverted pendulum mounted on the supporting foot. At the same time, it places the swing foot forward by moving the swing leg in a pendular arc, so that it makes the foot strike a ground when the mechanism is in a configuration identical to that at the beginning of a step. If the dynamic characteristic of the robot and the environment (e.g., the slope and velocity when the walking begins) agree, then the PDW robot achieves highly energy-efficient walking without any actuator control. Sugimoto [9] proposed a control method for quasi passive dynamic walking (Quasi-PDW). Quasi-PDW means that the robot usually does PDW without any input torque, and the actuators of the robot are used for ensuring walking stability only when the walking begins or when a disturbance occurs. Haruna [10] researched a PDW robot with a torso. CPG-based motion control inputs some torque to all the joints of the robot's lower limbs regardless of gait. When we think about human walking, we take into account the joints of the swing leg without any input torque. Active walking needs to be mixed with PDW for robot walking. Quasi-PDW is an example of a mixture of active walking and PDW. Quasi-PDW is applicable to the robot whose dynamic characteristic suits to PDW. However, there is a lot of robots that can not satisfy a dynamic characteristic for PDW. To achieve this mixture with the robots, we added the mechanism of PDW to an active walking robot. In this paper, we describe a motion control method based on the mixture of CPG and PDW, that is, the dynamic passivization of joint control, achieving robust and energy-efficient walking. We focused on robot walking on a downhill slope.

II. MOTION CONTROL METHOD

A. Link Model

The model of the human body is composed of the HAT (head, arms, and trunk), pelvis, thighs, shanks, and feet. There are seven joints, two each at the hips, knees, and ankles, and one at the trunk.

B. Neuro-Musculo-Skeletal System

In this research, we adopted the neuro-musculo-skeletal system [2] proposed by Taga for a motion control method based on CPG in the robot. The neuro-musculo-skeletal system is composed of two dynamical systems: a neural system and a musculo-skeletal system. In the neural system, the neural

978-1-4244-2794-9/09/$25.00 ©2009 IEEE

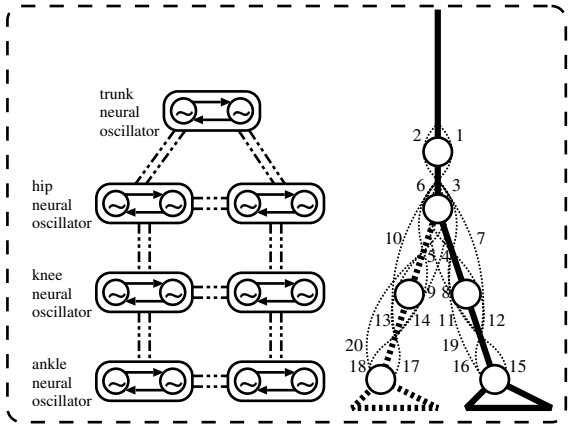

Fig. 1. Neuro-Musculo-skeletal system

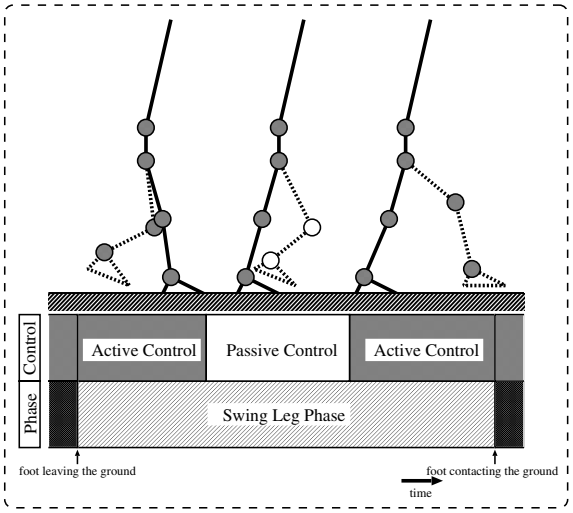

Fig. 2. Dynamic passivization of joint control

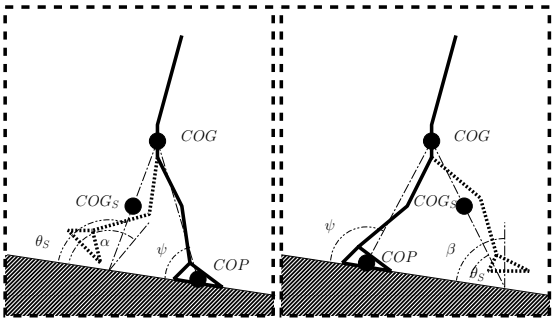

Fig. 3. Postures while walking

rhythm generator consists of seven neural oscillators in accordance with the robot's link structure. The neural oscillators are allocated to seven joints: the trunk and the pairs of the hips, knees, and ankles, shown in Fig. 1 (left). Two neurons at a neural oscillator each have a flexion and extension effect on muscles corresponding to the CPG. In the musculo-skeletal system, the skeletons match the robot's link structure. There are six single-joint muscles and three double-joint muscles for each of the limbs and two for the upper body. Fig. 1 (right) shows the configuration of the muscles. Two neurons in the neural oscillators alternately activate the antagonist muscles. The mathematical model of the neurons is represented in the following system of differential equations [1]:

$$\tau_i \dot{u_i} = -u_i - b \cdot f(v_i) + \sum_{j=1}^{n} w_{ij} f(u_j) + u_0 + S_i \quad (1)$$

$$\tau_i' \dot{v_i} = -v_i + f(u_i) \quad (2)$$

$$f(x) = max(x, 0), \quad (3)$$

where u_i is the inner state of the i-th neuron, v_i is a variable that represents the degree of adaptation or self-inhibition effect of the i-th neuron, τ and τ' are the time constants of the inner state and the adaptation effect of the i-th neuron, b is a coefficient of the adaptation effect, w_{ij} is a connecting weight from the j-th neuron to the i-th neuron, u_0 is an external input with a constant rate, and S_i is the local and global sensory information that is sent to the i-th neuron. A neuron excited by u_0 is oscillated by self-inhibition and cross-inhibition, and $f(u)$ is the output of the neuron.

C. Dynamic Passivization of Joint Control

In this paper, we describe a "Joint Control Transfer Switch" that is switched to "ACTIVE" or "PASSIVE" according to the environment and the posture information for adding the mechanism of PDW to the motion control method based on CPG. Our intention was to make the joint control of the swing leg temporarily passive in the swing leg phase. Fig. 2 shows a concept chart of the dynamic passivization of the joint control. The important part is the passive phase time and the switch timing of the joint control.

D. Joint Control Transfer Switch

The slope and posture information is used as information that decides the switch timing of the joint control (see Fig. 3). The body's center of gravity (COG) and the swing leg's center of gravity (COG_S) are obtained from the posture information while walking. Angle θ_S is calculated from the COG, COG_S, and the slope. In addition, angle ψ is calculated from the COG, center of pressure (COP), and the slope.

The joint control transfer switch changes joint control to active or passive according to the following conditions:

- $\psi \leq \frac{\pi}{2}$
  - $\theta_S \geq \alpha$: ACTIVE
  - $\theta_S < \alpha$: PASSIVE
- $\psi > \frac{\pi}{2}$
  - $\theta_S > \beta$: PASSIVE
  - $\theta_S \leq \beta$: ACTIVE,

where α and β are set to an appropriate value according to a dynamic characteristic of the robot and a slope ($0 \leq \alpha$, $\beta \leq \pi$).

E. Motion Control Based on Neuro-Musculo-Skeletal System

In this research, we added a joint control transfer switch (see Section II-D) to the neuro-musculo-skeletal system proposed by Taga for a motion control method. Fig. 4 shows a block diagram of the motion control system based on the dynamic passivization of joint control. If the transfer switch is passive, then it nullifies the input torque in the swing leg for the rhythmic torque controller and for the impedance torque controller. If it is active, then it enables the input torque in the swing leg for the rhythmic torque controller and for the impedance torque controller. The system performs the motion control based on the iteration of the following processes:

1) First, output $f(u(t))$ of the CPG in time t is excited by constant input u_0 to the neuron. The rhythmic torque controller generates rhythmic torque $T_{mr}(t+\Delta T)$ from $f(u(t))$, sensory input $S(t)$ of the robot at time t, and the output of the joint control transfer switch in time t.
2) The impedance torque controller generates impedance torque $T_{mi}(t+\Delta T)$ to maintain a standing position from joint angle $\theta(t)$, joint angular velocity $\dot{\theta}(t)$, and the sensory input of the robot at time t.
3) The muscle torque $T_m(t+\Delta T)$ is generated from $T_{mr}(t+\Delta T)$ and $T_{mi}(t+\Delta T)$.
4) The joint torque $T(t+\Delta T)$ is calculated from $T_m(t+\Delta T)$.
5) The kinematics simulator generates the motion of the robot when joint torque $T(t+\Delta T)$ is given to the robot. Then, the simulator calculates joint angle $\theta(t+\Delta T)$, joint angular velocity $\dot{\theta}(t+\Delta T)$, the coordinates $p(t+\Delta T) = (x(t+\Delta T), y(t+\Delta T))^T$, and velocity $\dot{x}(t+\Delta T)$, $\dot{y}(t+\Delta T)$ of each link after motion. The simulator sets the time forward for ΔT.
6) The flags of the foot contacting the ground S_{ron}, S_{roff}, S_{lon}, S_{loff} are obtained by the touch sense. The state of posture $S_g(t)$ is updated by them and by the output of the kinematics simulator.

III. WALKING EXPERIMENTS

We conducted a walking control experiment to test the effectiveness of our method. In the experiments, we used the neuro-musculo-skeletal system proposed by Taga and a control method where the joint control was set to passive during the swing leg phase for comparison with our method. The former method is labeled "*CPG*" and the latter method is labeled "*Passive*." Because this robot could not do PDW in this environment, PDW was excluded from the objects of comparison.

A. Optimizing Parameters

We optimized the common parameters of all the methods and parameters (α and β) of our method with simulated annealing with advanced adaptive neighborhood (SA/AAN) [11]

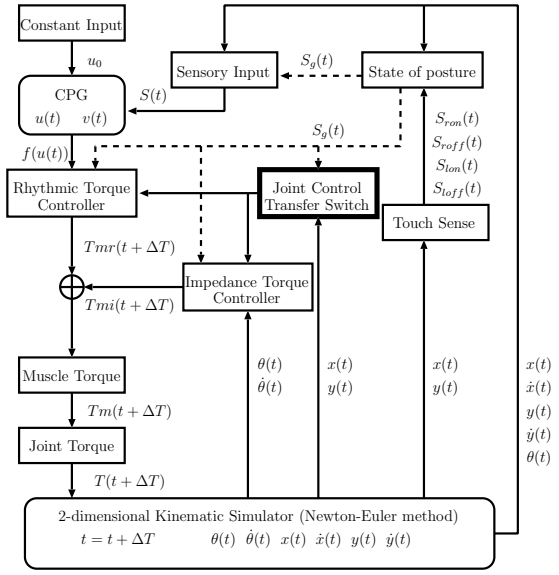

Fig. 4. Block diagram of motion control system based on dynamic passivization of joint control

prior to conducting the walking experiments (e.g., [4], [5]). We optimized the rhythmic torque parameter as common parameters of all the methods. The rhythmic torque Tmr_j that acts on j-th muscle is defined by the following equation:

$$Tmr_j = (r_{part} \cdot S_{on} + (1 - r_{part}) \cdot S_{off}) \cdot p_{part} \cdot f(u_i), \quad (4)$$

where r and p are rhythmic torque parameter, $part$ is a type of muscle, $S_{on}(S_{off})$ is flag of the contacting (leaving) the ground. In the experiments, the walking time and the locomotion cost were used for optimizing the performance. The value of the locomotion cost is defined by the following equation:

$$Cost \quad = \quad \frac{1}{L} \sum_{i=1}^{M} \int_0^{Time} |T_i(t)| dt, \quad (5)$$

where T_i is the input torque of the i-th joint, L is the travel distance, M is the number of joints, and $Time$ is the simulation time. We perturbed parameters 10,000 times simultaneously. Each simulation took 10 seconds. We set the value of reference [2] for the common parameters of all the methods other than rhythm torque parameter.

B. Generating Locomotion based on the Dynamic Passivization of Joint Control

First of all, we determined the effects of the dynamic passivization of the joint control. In this experiment, we used a 2 percent downhill slope.

Fig. 5 shows the gaits over 10 seconds on a 2 percent downhill slope. In this figure, the snapshots of the gait were traced every 0.3 seconds. Table I shows the travel distances,

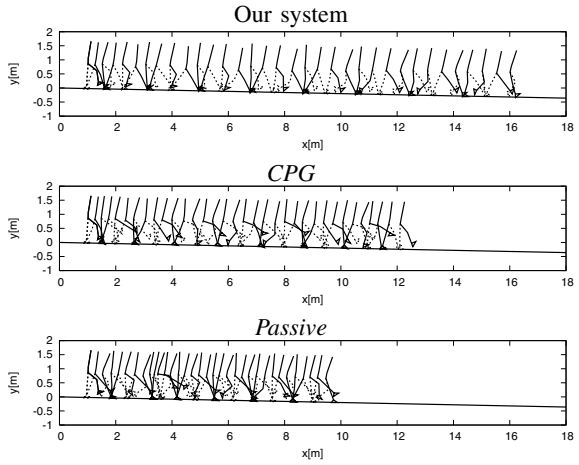

Fig. 5. Snapshots of gaits on 2 percent downhill slope with our system (top), *CPG* (middle), and *Passive* (bottom)

the sum total of the input torques, the locomotion costs, and the parameters of our method (α and β). Our system's walks were longer than the other's. Two methods, our system and the *Passive* system, having the mechanism of passivization of joint control generated walking that was more energy efficient than that of *CPG*. When our system is compared with the *Passive* system, we found that our system consumed more torque because its passive phase time was shorter. However, the travel distance increased more than the increment of the consumption torque, and our system reduced the locomotion cost.

C. Gait Stability Analysis

Next, we determined the gait stability. In this section, the two motion control methods of our system and *CPG* were used. In the following experiments, the *Passive* system was excluded from the comparison because it is a special example of our system and our system reduced the locomotion cost more than the *Passive* system in section III-B. Fig. 6 shows the phase plots of parts of the body in the frontal plane for 9.0 seconds from 1.0 second after the walking begins: the HAT (head, arms, and trunk) (top), the thigh of right leg (middle), and the shank of right leg (bottom). The horizontal axes represent the absolute angle in the radian, and the vertical axes represent the angular velocities. Our system generates steady periodic motion because its phase plots are more periodic than those of *CPG*.

We analyzed the gait stability using the maximum lyapunov exponent. Table II shows the maximum lyapunov exponent [12] of parts of the body. In this table, the maximum lyapunov exponents of our system's gait are smaller than those of *CPG*. The walking using our system is steadier than the *CPG*.

D. Adaptive Walking on Various Slopes

The performance of the systems on various downhill slopes was then examined at a 2 percent interval with a 0 to 18 percent

TABLE I
RESULTS OF FIRST EXPERIMENT

	Our system	*CPG*	*Passive*
Travel distance [m]	**15.4**	11.7	9.6
Sum total of input torque [Nms]	2.1E+03	2.2E+03	**1.6E+03**
Locomotion cost [Ns]	**1.4E+02**	1.9E+02	1.6E+02
α [rad]	1.79	-	-
β [rad]	0.24	-	-

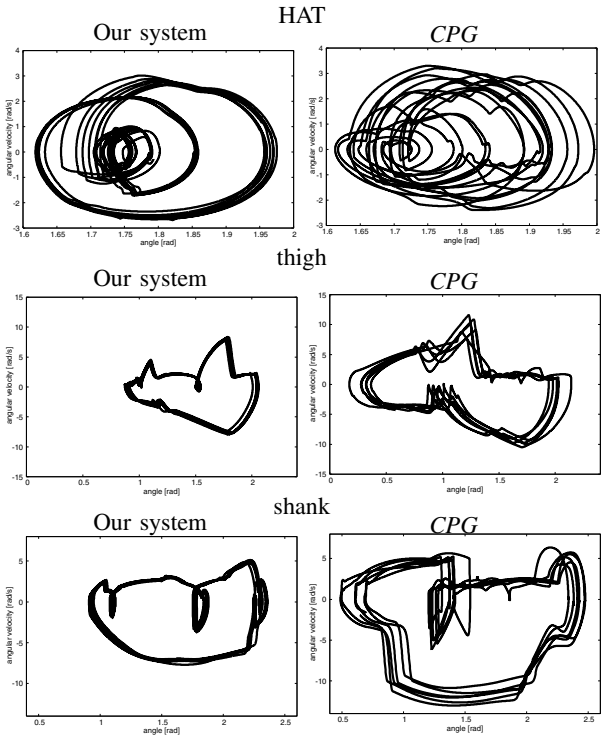

Fig. 6. Phase plots with our system (left) and *CPG* (right)

downhill slope. In this section, the parameters were optimized beforehand in each environment.

The experimental results demonstrated that our system and the *CPG* can walk for 10 or more seconds on downhill slopes with a 0 to 16 percent downhill. Our system and the *CPG* could not walk for 10 or more seconds on a 18 percent downhill slope. Fig. 7 shows the gaits over 10 seconds on a 16 percent downhill slope. In this figure, the snapshots of the gait were traced every 0.3 seconds. Our system walks farther than *CPG* on a 16 percent downhill slope, as the results in the preceding section also indicate. Fig. 8 shows the locomotion cost of each method on each downhill slope. Our system generates the energy-efficient walking on each downhill slope if it can walk for 10 or more seconds. Fig. 9 shows the parameters (α, β, the maximum value of θ_S (θ_S^{max}), and the minimum value of θ_S (θ_S^{min})) on each downhill slope. If α exceeds θ_S^{max} (14 and 16 percent downhill slopes), the joint control transfer switch changes the joint control to passive at the same time the foot leaves the ground. If β falls below θ_S^{min} (2, 10, 14, 16 percent

TABLE II
MAXIMUM LYAPUNOV EXPONENT

	Our system	*CPG*
$\lambda_{1\theta_1}$ (HAT)	**7.5E-02**	1.1E-01
$\lambda_{1\theta_2}$ (pelvis)	**9.3E-03**	1.3E-02
$\lambda_{1\theta_3}$ (right thigh)	**1.0E-01**	2.3E-01
$\lambda_{1\theta_4}$ (left thigh)	**1.6E-01**	2.3E-01
$\lambda_{1\theta_5}$ (right shank)	**1.2E-01**	2.7E-01
$\lambda_{1\theta_6}$ (left shank)	**2.2E-01**	2.4E-01
$\lambda_{1\theta_7}$ (right foot)	**1.0E-01**	1.5E-01
$\lambda_{1\theta_8}$ (left foot)	1.7E-01	**1.4E-01**
average	**1.2E-01**	1.7E-01

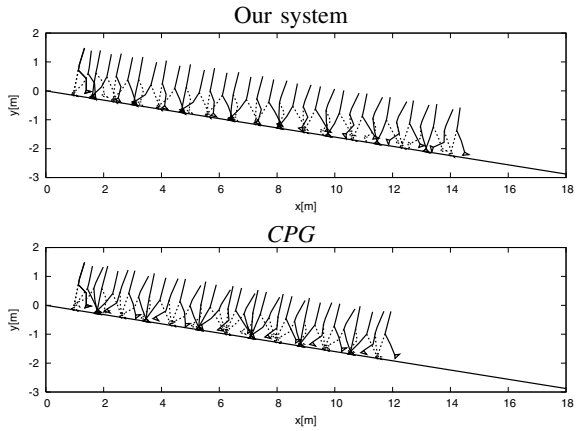

Fig. 7. Snapshots of gaits on 16 percent downhill slope with our system (top) and *CPG* (bottom)

downhill slope), the joint control transfer switch changes the joint control to active at the same time as the foot touches the ground. Our system generates energy-efficient walking on various (from 0 to 12 percent) downhill slopes because it uses the passive phase appropriately. Our system generates walking that has been made passive on a 14 or 16 percent downhill slope for all periods of the swing leg phase.

E. Adaptive Walking on Uneven Terrain

Next, we conducted a walking control experiment on uneven terrain. The profile of the downhill slope $y_g(x)$ is described by

$$y_g(x) = \begin{cases} -0.02x & (x < x_0) \\ -a(x - x_0) - 0.02x_0 & (x \geq x_0), \end{cases} \quad (6)$$

where a ($0 \leq a \leq 4$) is the slope of the terrain at a 0.0025 interval, and x_0 is the position at which the slope of the terrain changes. In this experiment, we set $x_0 = 5$. We used each parameter that was obtained in the preceding section. Table III shows the experimental results. In this table, "✓" indicates that the robot could walk for 10 or more seconds. "×" means that the robot could not walk for 10 or more seconds; it fell down. Our system has robustness that is as good as *CPG*'s on uneven terrain. We found that our system did not detract from the robustness of CPG. Fig. 10 shows the gaits over 10 seconds; $a = 0.0325$. In this figure, the snapshots of the gaits

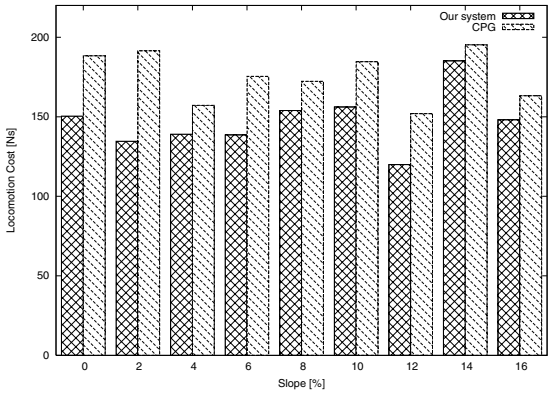

Fig. 8. Locomotion costs

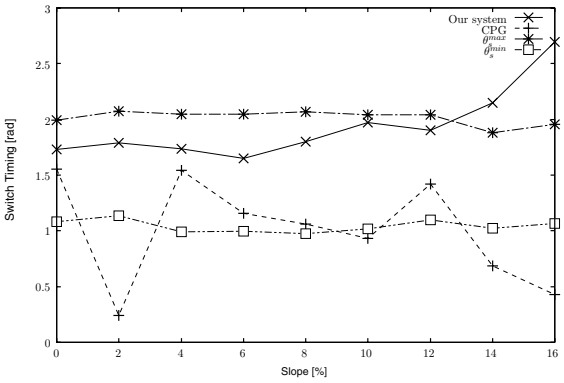

Fig. 9. Parameters of our method

are traced every 0.3 seconds. Our system performs gaits that are more stable than those of *CPG*.

F. Comparing Robot Gait with Human Gait

Finally, we compared the robot and human gaits. The data on the human gait were measured using motion capture.

Fig. 11 shows the gait over 2 seconds on a 14 percent

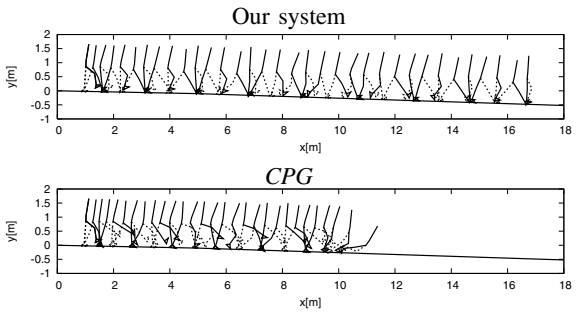

Fig. 10. Snapshots of gaits on uneven terrain with our proposed (top) and *CPG* (bottom)

TABLE III
RESULTS OF WALKING EXPERIMENT ON UNEVEN TERRIAN

a	variation	Our system	*CPG*
0	-0.0200	✓	✓
0.0025	-0.0175	✓	✓
0.0050	-0.0150	✓	✓
0.0075	-0.0125	✓	✓
0.0100	-0.0100	✓	×
0.0125	-0.0075	✓	✓
0.0150	-0.0050	✓	✓
0.0175	-0.0025	✓	×
0.0200	0	✓	×
0.0225	0.0025	✓	×
0.0250	0.0050	✓	×
0.0275	0.0075	✓	✓
0.0300	0.0100	✓	✓
0.0325	0.0125	✓	×
0.0350	0.0150	×	×
0.0375	0.0175	×	×
0.0400	0.0200	×	×

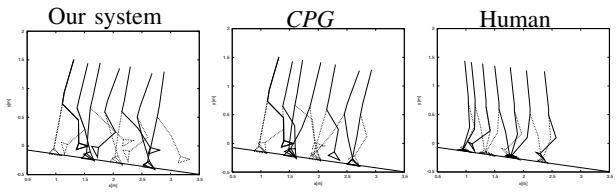

Fig. 11. Snapshots of gaits on 14 percent downhill slope with our system (left), *CPG* (center), and Human (right)

downhill slope. In this figure, the snapshots of the gait were traced every 0.3 seconds. The our system's and *CPG*'s gaits are vorlage. In contrast, human's gait is backward tilting.

The error of the vertical component of the COG's trajectory for the robot gait and that for the human gait were calculated. Fig. 12 shows the trajectories of the COG. In this figure, the trajectory of our system's gait is closer to the trajectory of a human gait than the *CPG*'s, and it is more periodically steady than *CPG*'s as well. The mean absolute error of our system is 0.0122[m], and that of *CPG* is 0.0285[m]. Our system's gait is closer to a human gait than *CPG*'s.

IV. CONCLUSIONS AND FUTURE WORK

We described a motion control method based on a mixture of CPG and PDW, that is, dynamic passivization of joint control. We conducted walking control experiments to test the effectiveness of our method, and it demonstrated superior gaits. In gait stability analysis, we conducted that our system generated more stable gait than *CPG*'s. We conducted walking control experiments on various downhill slopes, and our method was superior here as well. In experiments on uneven terrain, our method generated robust walking that was better than *CPG*'s. We compared the robot and human gait, and our system had a trajectory that more closely modeled human walking than *CPG*.

In future work, we will create a motion control method that accounts for dynamic passivization of joint control other than in the swing leg. We will analyze the factor that the

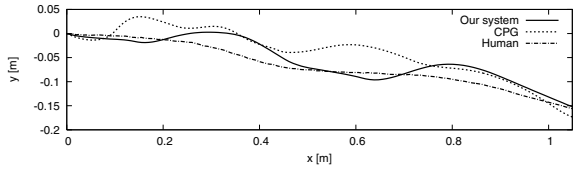

Fig. 12. Trajectories of COG

motion control using our system improved gait stability and robustness.

ACKNOWLEDGMENTS

We are grateful to Chukyo University for measurement of human walking using motion capture in Motion Analysis Lab. This work was supported in part by the Ministry of Education, Science, Sports and Culture, Grant–in–Aid for Scientific Research under grant #17500143 and #20700199, and by the Tatematsu Foundation.

REFERENCES

[1] G. Taga, Y. Yamaguchi, and H. Shimizu, "Self-organized control of bipedal locomotion by neural oscillators in unpredictable environment", *Biological Cybernetics*, Vol. 65, pp. 147-159, 1991.

[2] G. Taga, "A model of the neuro-musculo-skeletal system for human locomotion I. Emergence of basic gait", *Biological Cybernetics*, Vol. 73, pp. 97-111, 1995.

[3] G. Taga, "A model of the neuro-musculo-skeletal system for human locomotion II. Real-time adaptability under various constraints", *Biological Cybernetics*, Vol. 73, pp. 113-121, 1995.

[4] Y. Itoh, K. Taki, S. Kato, and H. Itoh, "A Stochastic Optimization Method of CPG-based Motion Control for Humanoid Locomotion", In *IEEE Conference on Robotics, Automation and Mechatronics (RAM'2004)*, pp. 347-351, 2004.

[5] K. Taki, Y. Itoh, S. Kato, and H. Itoh, "Motion Generation for Bipedal Robot Using Neuro-musculo-skeletal Model and Simulated Annealing", In *IEEE Conference on Robotics, Automation and Mechatronics (RAM'2004)*, pp. 699-703, 2004.

[6] S. Miyakoshi, G. Taga, Y. Kuniyoshi, and A. Nagakubo, "Three dimensional bipedal stepping motion using neural oscillators - towards humanoid motion in the real world -", In *Proceedings of the 1998 IEEE/RSJ International Conference on Intelligent Robots and Systems (IROS'98)*, Vol. 1, Victoria Conference Center (Victoria), IEEE Service Center, pp. 84-89., 0-7803-4465-0, 1998.

[7] S. Kotosaka, and S. Schaal, "Synchronized robot drumming by neural oscillators", In *Proceedings of the International Symposium on Adaptive Motion of Animals and Machines*, Montreal, Canada, August 8-12, 2000.

[8] T. McGeer, "Passive Dynamic Walking", *The International Journal of Robotics Research*, Vol. 9, No. 2, pp. 62-81, 1990.

[9] Y. Sugimoto and K. Osuka, "Walking Control of Quasi Passive Dynamic Walking Robot "Quartet III" based on Continuous Delayed Feedback Control", In *Proceedings of IEEE International Conference on Robotics and Biomimetics (Robio 2004)*, Shenyang, China, 2004, August.

[10] M. Haruna, M. Ogino, K. Hosoda, and M. Asada, "Yet Another Humanoid Walking. -Passive Dynamic Walking with Torso under Simple Control-", In *Proceedings of the 2001 IEEE/RSJ International Conference on Intelligent Robots and Systems*, CD-ROM, 2001.

[11] M. Miki, T. Hiroyasu, and K. Ono, "Simulated Annealing with Advanced Adaptive Neighborhood", In *Proceedings of the 2nd International Workshop on Intelligent Systems Design and Applications (ISDA 2002)*, pp. 113-118, 2002.

[12] Kathleen T. Alligood, Tim D. Sauer, and James A. Yorke, "Chaos: an introduction to dynamic systems", In *Springer*, 1996.